CrossMark

ORIGINAL ARTICLE

Identification of AB-FUBINACA metabolites in human hepatocytes and urine using high-resolution mass spectrometry

Marisol S. Castaneto[1,2] · Ariane Wohlfarth[1] · Shaokun Pang[3] · Mingshe Zhu[4] ·
Karl B. Scheidweiler[1] · Robert Kronstrand[5,6] · Marilyn A. Huestis[1]

Abstract AB-FUBINACA, *N*-(1-amino-3-methyl-1-oxobutan-2-yl)-1-(4-fluorobenzyl)-1*H*-indazole-3-carbox-amide, is an indazole synthetic cannabinoid identified in drug seizures around the world. Few metabolism data are available, despite the need for human urinary markers to detect AB-FUBINACA intake. Our main objective was to identify suitable analytical targets by analyzing human hepatocyte incubation samples with high-resolution mass spectrometry (HRMS) and to confirm the results in authentic urine specimens. We also determined AB-FUBINACA's metabolic stability in human liver microsomes (HLMs) and compared hepatocyte and urine results with in silico predictions. The metabolic stability of AB-FUBINACA was determined in pooled HLMs (1 μmol/l, up to 1 h). The metabolite profile of human hepatocytes (10 μmol/l, 1 and 3 h) and urine samples from two subjects were determined by HRMS using information-dependent tandem-mass spectrometry (MS-MS) acquisition. Data were analyzed with MetabolitePilot™ software utilizing different processing algorithms, including generic peak finding, mass defect filtering, neutral loss, and product ion filtering. In silico metabolite prediction was performed with MetaSite™ software. AB-FUBINACA's half-life in HLMs was 62.6 ± 4.0 min. AB-FUBINACA produced 11 metabolites (2 glucuronides) in human hepatocytes and 10 were identified in authentic human urine. Major metabolic pathways were terminal amide hydrolysis, acyl glucuronidation and hydroxylation at the aminooxobutane moiety. Epoxidation followed by hydrolysis, hydroxylation at the indazole moiety and dehydrogenation were minor pathways. Defluorination did not occur. Seventeen first-generation metabolites were predicted in silico, of which seven were observed in vitro and eight in vivo. We recommend AB-FUBINACA carboxylic acid, hydroxy AB-FUBINACA carboxylic acid, dihydrodiol AB-FUBINACA and dihydrodiol AB-FUBINACA carboxylic acid as suitable urinary markers.

Keywords AB-FUBINACA · Metabolite profiling · HRMS · Hepatocytes · In silico

✉ Marilyn A. Huestis
mhuestis@intra.nida.nih.gov

1 Chemistry and Drug Metabolism, Intramural Research Program, National Institute on Drug Abuse, National Institutes of Health, 251 Bayview Boulevard, Suite 200 Room 05A-721, Baltimore, MD 21224, USA

2 Program in Toxicology, University of Maryland, School of Medicine, Baltimore, MD, USA

3 SCIEX, Redwood City, CA, USA

4 Department of Biotransformation, Bristol-Myers Squibb, Research and Development, Princeton, NJ, USA

5 Department of Forensic Genetics and Forensic Toxicology, National Board of Forensic Medicine, Linköping University, Linköping, Sweden

6 Division of Drug Research, Department of Medical and Health Sciences, Linköping University, Linköping, Sweden

Introduction

Synthetic cannabinoids were originally synthesized to investigate the endocannabinoid system or for their potential therapeutic benefits, but none progressed to clinical use [1]. Many synthetic cannabinoids are potent CB$_1$ agonists eliciting cannabimimetic effects similar to plant-derived delta-9-tetrahydrocannabinol (THC). Synthetic cannabinoids have been the most commonly identified new psychoactive substances in the recreational drug market since

Springer

they were first introduced in the early 2000s and are abused for their psychoactive effects [2]. The US Synthetic Drug Abuse Prevention Act of 2012 placed many synthetic cannabinoids under Schedule I [3], but clandestine laboratories circumvent regulations by modifying compounds.

AB-FUBINACA, N-(1-amino-3-methyl-1-oxobutan-2-yl)-1-(4-fluorobenzyl)-1H-indazole-3-carboxamide, was first developed by Pfizer as a potent CB_1 agonist ($EC_{50} = 28$ nM and $K_i = 0.9$ nM) [4] compared to THC ($EC_{50} = 167 \pm 84$ nM and $K_i = 15.3 \pm 4.5$ nM) [5]. AB-FUBINACA has an indazole core with a 4-fluorobenzyl moiety and a carboxamide-linked aminooxobutane moiety (Fig. 1). It was first detected in Japan in 2012 [6], in the US in 2013 [7], and scheduled by the US Drug Enforcement Administration (DEA) in early 2014 [8]. There are no controlled drug administration studies on AB-FUBINACA investigating its directly linked adverse effects. However, several hospitalizations following intake of a structurally similar indazole carboxamide, ADB-PINACA [9], have occurred; this compound produced nausea and vomiting, seizures, somnolence, hyperglycemia, hyperkalemia, tachycardia, myocardial infarction, pneumonia and rhabdomyolysis. Fatalities and numerous hospitalizations were due to consumption of the methyl ester of AB-FUBINACA carboxylic acid according to the Russian Federal Drug Control Service [10]. In rare cases, other synthetic cannabinoids produced kidney toxicity and/or death [1, 11]. Drug user forums can help in assessing a compound's effects, although user reports are subjective and might be inaccurate since individuals cannot verify the package's content [12].

Identification and quantification of synthetic cannabinoids and metabolites in biological matrices are critical for documenting intake and correlating toxicity to analyte concentrations. Parent synthetic cannabinoids can be identified in blood, oral fluid, and hair, whereas metabolites are predominantly identified in urine and extend the

window of detection [11]. Due to limited pharmacology, toxicity and safety data, controlled in vivo human pharmacokinetic studies are not possible, with data being confined to self-administered experiments [1]. In vivo animal [13–15], in vitro human liver microsomes (HLMs) [15–19], and in vitro human hepatocyte experiments [20–24] provide alternative approaches, which can be supplemented by in silico metabolite prediction [25].

Currently, AB-FUBINACA metabolism data are limited. After AB-FUBINACA incubation with HLMs, Takayama et al. [16] reported a single metabolite hydroxylated at the aminooxobutane moiety. Thomsen et al. [26] found AB-FUBINACA carboxylic acid and hydroxy AB-FUBINACA metabolites following incubation with HLMs and identified carboxylesterase 1 as the major enzyme responsible for amide hydrolysis. Our aims were to determine AB-FUBINACA metabolic stability with HLMs, identify AB-FUBINACA phase I and II metabolism after human hepatocyte incubation by high-resolution mass spectrometry (HRMS), and to confirm metabolites in authentic urine specimens. Additionally, we assessed the utility of the in silico metabolite prediction software MetaSite^{TM}.

Materials and methods

Chemical and reagents

AB-FUBINACA (98.4 % purity) was generously donated by the DEA Special Testing and Research Laboratory. The AB-FUBINACA stock solution was prepared by dissolving the compound in dimethyl sulfoxide (DMSO). Pooled ($n = 10$) cryopreserved human hepatocytes, pooled HLMs ($n = 50$), thawing and incubation media, Krebs-Henseleit buffer (KHB), and nicotinamide adenine dinucleotide phosphate (NADPH)- regenerating solutions were obtained from BioreclamationIVT (Baltimore, MD, USA). Acetonitrile and ethyl acetate were purchased from Sigma-Aldrich (St. Louis, MO, USA). Potassium phosphate, glacial acetic acid, and formic acid were acquired from Fisher Scientific (Waltham, MA, USA). All reagents were high performance liquid chromatography (HPLC) grade or better. Isolute (1 ml) supported liquid extraction (SLE+) columns (Biotage, Inc., Charlotte, NC, USA) were utilized in sample preparation. Water was purified in-house by an ELGA Purelab Ultra Analytic purifier (Siemens Water Technologies, Lowell, MA, USA). Diclofenac was obtained from Cayman Chemical (Ann Arbor, MI, USA).

Metabolic stability assessment with HLMs

HLM experiments were performed in duplicate by incubating 1 μmol/l AB-FUBINACA in 1 mg/ml HLM
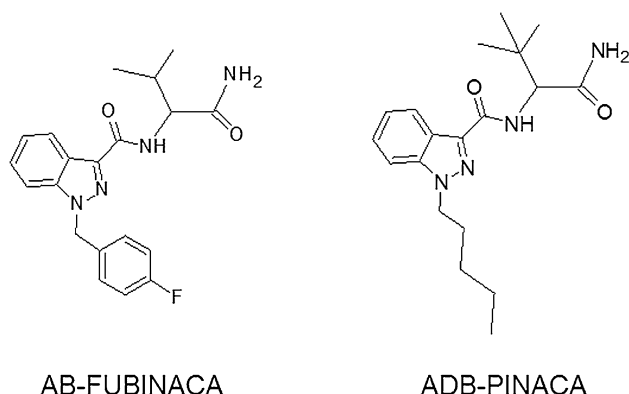

Fig. 1 Chemical structures of AB-FUBINACA and its analog, ADB-PINACA

suspensions prepared in a final volume of 1 ml with 50 mmol/l potassium phosphate buffer (pH 7.4) and an NADPH regenerating system (glucose-6-phosphate, $MgCl_2$ and glucose-6-phosphate dehydrogenase). The organic AB-FUBINACA stock solution was diluted with phosphate buffer to 1 µmol/l; the final organic content was <0.04 %. Samples were gently mixed, incubated at 37 °C for up to 1 h in a shaking water bath, and the reaction was stopped by mixing 100 µl of incubation sample with 100 µl of ice cold acetonitrile after 0, 3, 8, 13, 20, 30, 45, and 60 min. Samples were centrifuged at 15,000 g, 4 °C for 5 min and supernatants stored at −80 °C before analysis. For liquid chromatography–tandem mass spectrometry (LC–MS-MS) analysis, samples were thawed and centrifuged at 15,000 g, 4 °C for 5 min. A 1:100 supernatant dilution was prepared in mobile phases A and B (90:10, v/v) and 10 µl was injected onto the LC–MS-MS system.

Chromatographic separation was performed on a Kinetex^{TM} C18 column (100 mm × 2.1 mm, 2.6 µm) fitted with a KrudKatcher Ultra HPLC in-line filter (0.5 µm × 0.1 mm i.d.; Phenomenex, Torrance, CA, USA) and on a Shimadzu (Columbia, MD, USA) HPLC system with two LC-20AD$_{xr}$ pumps, a DGU-20AR degasser, a SIL-20AC$_{xr}$ autosampler, and a CT20A column oven equipped with the Kinetex C18 column. The HPLC mobile phase consisted of 0.1 % formic acid in water (A) and 0.1 % formic acid in acetonitrile (B). Column and autosampler temperatures were set at 40 and 4 °C, respectively. A 0.3 ml/min flow rate was maintained with 10 % B for 0.3 min, ramped to 55 % B at 20.0 min, increased to 95 % B at 20.1 min for 1.8 min, then 10 % B at 22 min, for a total 25 min run time. Positive electrospray ionization (ESI) mass spectrometry (MS) analysis was performed on a 5500 QTRAP (SCIEX, Redwood City, CA, USA) with data acquired via SCIEX Analyst software (version 1.6) in multiple reaction monitoring (MRM) mode. Two MRM transitions for AB-FUBINACA (target: 369.2 → 253.1; qualifier 369.2 → 324.2) were monitored. Declustering potential, entrance potential, exit potential and collision energy were optimized to 80 V, 10 V, 10 V, 35 eV (target) and 23 eV (qualifier), respectively.

AB-FUBINACA peak areas were plotted against time and used to calculate in vitro microsomal half-life ($T_{1/2}$) and intrinsic clearance ($CL_{int, \ micr}$) according to Baranczewski et al. [27]. The microsomal intrinsic clearance was scaled to whole liver dimensions according to McNaney et al. [28], yielding intrinsic clearance (CL_{int}). Human hepatic clearance (CL_H) and extraction ratio, excluding plasma protein binding parameters, also were calculated [27].

Metabolite profiling in human hepatocytes

Hepatocyte incubations were performed as previously published [20]. AB-FUBINACA (10 µmol/l) was incubated with cryopreserved human hepatocytes (5×10^5 cells/ 0.5 ml/well) with ≥80 % cell-viability. The stock solution was dissolved in Krebs-Henseleit buffer (KHB) to a final concentration of 20 µmol/l, yielding an organic solvent percentage in the hepatocyte incubation of <0.7 %. To confirm pooled hepatocyte enzymatic activity, 10 µmol/l diclofenac (CYP2C9 substrate) served as a positive control. Cells were incubated at 37 °C under constant gentle shaking. Reactions were stopped with 0.5 ml ice-cold acetonitrile after 0, 1, and 3 h. After centrifugation, supernatants were removed and stored at −80 °C. For analysis, hepatocytes samples were thawed and centrifuged at 15,000 g, and 4 °C for 10 min. Supernatants were diluted 1:5 in mobile phase and 25 µl was injected onto the LC-time-of-flight (TOF) system, and the supernatants were also subjected to SLE+ with and without enzymatic hydrolysis before the LC–TOF-MS analysis in addition to only dilution of the supernatants.

HPLC separations were performed on a Shimadzu Prominence^{TM} system outfitted with two LC-20AD$_{xr}$ pumps, a DGU-20A5R degasser, a SIL-20AC$_{xr}$ autosampler and a CTO-20AC column oven. HPLC column, mobile phases, and gradient conditions utilized in the half-life determination were employed. Column and autosampler temperatures were held at 40 and 4 °C, respectively. MS analysis was performed on a 5600+ Triple TOF mass spectrometer (SCIEX) with data acquired via SCIEX Analyst TF software (version 1.6). MS and MS-MS data were acquired in positive ESI mode with information-dependent acquisition (IDA) and dynamic background subtraction. For IDA, TOF-MS signals exceeding 500 cps were selected for the dependent scan (exclusion of isotopes within 3 Da; mass tolerance ± 50mDa). TOF-MS were acquired within an m/z 100–950 mass range followed by product ion scans at m/z 60–950 with accumulation times of 0.1 and 0.075 s, respectively. Declustering potential and collision energy were optimized via infusion and were 80 V and 32 ± 18 eV, respectively. Calibrators were injected every third injection.

Metabolites were detected by data mining with MetabolitePilot^{TM}, (SCIEX, version 1.5) employing multiple peak finding algorithms, which included scanning for predicted metabolites, generic peak finding, mass defect filtering, and product ion and neutral loss filterering that targeted at least two characteristic commonly produced ions or neutral losses. The extracted ion chromatogram peak intensity threshold was set at 1500 cps with minimum MS and MS-MS peak

intensities of 400 and 100 cps, respectively. Structures of potential AB-FUBINACA metabolites were determined based on mass shift, fragmentation patterns, and retention time. Possible adduct formation or in-source collision-induced dissociation or water loss were excluded from the final metabolite list.

Metabolite profiling in authentic human urine specimens

We analyzed two urine samples collected from individuals suspected of driving under the influence of drugs, provided by the National Board of Forensic Medicine in Linköping, Sweden. We analyzed the matching urine specimens from two blood samples containing 9 and 42 ng/g AB-FUBINACA. Hepatocytes and urine samples were prepared with and without enzymatic hydrolysis. In separate tubes, 250 μl of urine and 50 μl of hepatocyte samples were diluted with 600 and 800 μl of 0.4 mol/l ammonium acetate buffer (pH 4.0), respectively. Beta glucuronidase from Red Abalone (40 μl, 15,625 IU/ml; BG100™ from Kura Biotec, Chile) was added and samples were incubated at 55 °C for 1 h. Subsequently, 200 μl of cold acetonitrile was added followed by centrifugation at 15,000 g and 4 °C for 10 min. Samples were loaded onto SLE+ columns and eluted twice with 3 ml of ethyl acetate. Extracts were dried under nitrogen at 42 °C, reconstituted in 150 μl of mobile phase and analyzed under the LC–TOF-MS conditions utilized in the metabolite profiling.

Peak areas for metabolites previously identified in hepatocytes were monitored with MultiQuant software (SCIEX). We also processed urine specimen data with MetabolitePilot™ data mining procedures. Data review and processing included identification of metabolites previously identified in hepatocyte samples and identification of the overall top 20 most intense metabolites in authentic urine (molecular weight > 250 Da, ≤ ± 5 ppm mass measurement accuracy), whether present or not in the hepatocyte samples.

In silico prediction of AB-FUBINACA metabolism

AB-FUBINACA metabolism was predicted with MetaSite™ software (version 5, Molecular Discovery Ltd, Pinner, UK). Potential hepatic metabolites were predicted with a list of 39 common cytochrome P450 biotransformations, including hydroxylation, dealkylation, carbonylation and dehalogenation. For each potential metabolite, the software assigned a probability score representing the likelihood of the metabolite being generated, with 100 % being the maximum score. Only metabolites >150 Da were included in the final summary.

The most probable second-generation metabolites were predicted for the top three first-generation metabolites.

Results

Metabolic stability of AB-FUBINACA in HLMs

AB-FUBINACA half-life ($T_{1/2}$) was 62.6 ± 4.0 min, in vitro microsomal intrinsic clearance ($CL_{int, micr}$) was 11.0 μl min^{-1} mg^{-1} and intrinsic clearance (CL_{int}) was 10.5 ml min^{-1} kg^{-1}. Hepatic clearance CL_H was predicted as 6.9 ml min^{-1} kg^{-1} with an extraction ratio of 0.34.

Metabolic profiling of AB-FUBINACA in human hepatocytes

In the control, diclofenac concentration decreased by 90 % after 3-h incubation. In addition, time-dependent concentration increases of 4′-hydroxydiclofenanc and diclofenac β-D-acyl glucuronide confirmed active hepatocyte enzymatic activity. We identified 11 AB-FUBINACA metabolites, nine phase I metabolites (M1, M3, M4, M5, M6, M7, M9, M10, and M11) and two phase II metabolites (M2 and M8) with mass measurement accuracy ≤2.0 ppm in the 3-h hepatocyte sample (Table 1). M4, M6, M8, M9, and M11 were also detected in the 1-h sample. Metabolic reactions included terminal carboxamide hydrolysis (M11), epoxidation followed by hydrolysis (M1), hydroxylation (M3–M6), dehydrogenation (M9), and reaction combinations (M7, M10). Glucuronide conjugation of M11 produced M8, and glucuronidation of a monohydroxylated phase I metabolite generated M2. No defluorinated metabolite was observed. Based on MS peak areas, M11 and M6 were the two most intense metabolites. Retention times, accurate masses, mass errors, peak areas, and characteristic fragments of AB-FUBINACA and metabolites are summarized in Table 1. Figure 2a, b exhibits metabolite profiles in human hepatocytes.

Metabolite confirmation and profiling in authentic urine specimens

All metabolites were detected in the hepatocyte samples subjected to SLE+ preparation with only minimal analyte loss when compared to the diluted 3-h hepatocyte samples (Table 2; Fig. 2). Beta-glucuronidase successfully cleaved M2, but M8 hydrolysis was less efficient. All AB-FUBINACA metabolites previously identified in hepatocyte samples were also found in both authentic urine specimens, except for M9 (Fig. 2c, d). As we observed for hepatocytes, M11 was the most predominant metabolite in both urine specimens. Overall, metabolite prevalences were similar to what was observed in the hepatocyte samples and similar for both authentic urine specimens. Only prevalences for M6 (intensity↓), M7 (↑) and M8 (↑) differed when compared to the hepatocyte profile (Table 2).

Table 1 Retention time (RT), elemental composition, accurate mass protonated ion ([M + H]$^+$, *m/z*), diagnostic product ions, mass error and peak areas (1 and 3 h) of AB-FUBINACA, and its metabolites in human hepatocyte samples

Peak ID	Metabolic reaction	RT (min)	Elemental composition	[M + H]$^+$ (*m/z*)	Diagnostic product ions (*m/z*)	Mass error (ppm)	Peak area (1 h)	Peak area (3 h)	Rank
M1	Epoxide hydrolysis	8.81	$C_{20}H_{23}N_4O_4F$	403.1774	109, 241, 269, 287, 358, 386	0.4	ND	1.47E+04	6
M2	Hydroxylation + glucuronidation	9.45	$C_{26}H_{29}N_4O_9F$	561.1985	269, 340, 445, 516, 544	−1.2	ND	1.09E+04	9
M3	Dihydroxylation	12.57	$C_{20}H_{21}N_4O_4F$	401.1618	109, 253, 326, 356,384	−0.3	ND	6.80E+03	10
M4	Hydroxylation	12.99	$C_{20}H_{21}N_4O_3F$	385.1674	109, 269, 340, 368	0.6	8.30E+03	1.58E+04	5
M5	Hydroxylation	13.50	$C_{20}H_{21}N_4O_3F$	385.1670	109, 253, 340, 368	0.0	ND	1.41E+04	8
M6	Hydroxylation	13.68	$C_{20}H_{21}N_4O_3F$	385.1674	109, 253, 310, 340, 368	1.5	1.56E+05	3.63E+05	2
M7	Hydroxylation + amide hydrolysis	14.77	$C_{20}H_{20}N_3O_4F$	386.1514	109, 253, 350, 368	0.0	ND	3.80E+04	4
M8	Amide hydrolysis + glucuronidation	14.98	$C_{26}H_{28}N_3O_9F$	546.1876	109, 253, 324, 352, 370, 528	−1.2	1.77E+04	8.98E+04	3
M9	Dehydrogenation	15.96	$C_{20}H_{19}N_4O_2F$	367.1563	109, 253, 322, 350	−0.5	5.23E+03	1.46E+04	7
M10	Amide hydrolysis + dehydrogenation	17.67	$C_{20}H_{18}N_3O_3F$	368.1398	109, 253, 322, 350	−1.8	ND	3.72E+03	11
M11	Amide hydrolysis	18.31	$C_{20}H_{20}N_3O_3F$	370.1568	109, 253, 324	2.0	1.27E+06	3.00E+06	1
	AB-FUBINACA	16.17	$C_{20}H_{21}N_4O_2F$	369.1778	109, 253, 324, 352	1.4	3.81E+06	2.96E+06	

Peak area for AB-FUBINACA parent at time 0 h was 5.17E+06. Metabolites in the 3-h sample are ranked by most to least intense peak areas. Each sample was analyzed once.

ND not detected

In specimen 1, the most intense metabolites were M11, M7, and M8 while M1–M6 and M10 were minor metabolites. Enzymatic hydrolysis increased M1, M3, M4, M5, M7, and M11 peak areas between 25 and 920 %. Notably, a small signal for the AB-FUBINACA parent was detected in this urine specimen.

In specimen 2, the most intense metabolites, again, were M11, M7, M8, and M1 with M2–M6 and M10 being minor, with no parent detectable. Especially, M1 and M4 peak areas increased after hydrolysis (64–88 %); only slight increases were observed for M6 and M7 (11–20 %).

Results for the top 20 most intense metabolites in authentic urine samples are shown in Table 3 and Fig. 3. At least six of the eleven metabolites identified in the hepatocytes were also among these top 20 metabolites. Still, M11, M7, and M8 were the three most intense metabolites followed by dihydrodiol AB-FUBINACA carboxylic acid (metabolite g, Table 3) and a metabolite generated by loss of the fluorobenzyl moiety (*N*-dealkylation) and hydroxylation (metabolite a, Table 3). Many additional metabolites not observed in the hepatocytes were identified in the urine and were generated by combination of dihydroxylation (f, i), epoxidation followed by hydrolysis with hydroxylation (c) or terminal amide hydrolysis (g), terminal amide hydrolysis with hydroxylation (d, u, x, y) or dihydroxylation (o) with glucuronidation (k, l, n, p, q) or dehydrogenation (z). Carboxylation (m), internal amide hydrolysis (j) with hydroxylation of the fluorobenzylindazole (w), internal

carboxamide hydrolysis with hydrogenation (s), *N*-dealkylation of aminooxobutane (t) with hydroxylation (e, h), and *N*-dealkylation of fluorobenzyl with hydroxylation (a) or dehydrogenation (b) also were observed. We identified metabolite "v" as another M8 isomer, whereas metabolite "r" was glucuronidated AB-FUBINACA with an unassigned structure.

In silico prediction

MetaSite^{TM} predicted 17 potential metabolites with 10 metabolites (P1–P10) scoring ≥20 % (Table 4). The top three candidates, all scoring 100 %, were products of aliphatic hydroxylation or dehydrogenation at the 2″-position of the aminooxobutane moiety or dealkylation of the aminooxobutane moiety. Other predicted metabolites were products of hydroxylation at the fluorobenzyl methylene carbon, aminooxobutane moiety or indazole moiety, *N*-dealkylation of the fluorobenzyl moiety or aliphatic carbonylation at the fluorobenzyl methylene carbon. Defluorination was not predicted.

Second-generation metabolites of the top three first-generation metabolites (P1, P2, and P3) scoring 100 % were generated by hydroxylation at the aminooxobutane (P3a) or methylene carbon of fluorobenzyl (P1a and P2a), *N*-dealkylation (loss of fluorobenzyl, P1b and P2b), carbonylation (P1c, P2c, and P3c), carboxylation (P3d), and dehydrogenation (P3b). Results are also listed in Table 4.

Fig. 2 Combined extracted ion chromatograms of AB-FUBINACA and its metabolites identified in hepatocyte samples and authentic urine specimens. Signals obtained after enzymatic hydrolysis are shown in broken lines. **a** 3-h Hepatocyte sample, 1:5 diluted. **b** 3-h Hepatocyte sample with and without enzyme hydrolysis treatment and solid-supported liquid extraction (SLE+). **c** Authentic urine specimen 1 with or without hydrolysis and SLE+. **d** Authentic urine specimen 2 with or without hydrolysis and SLE+
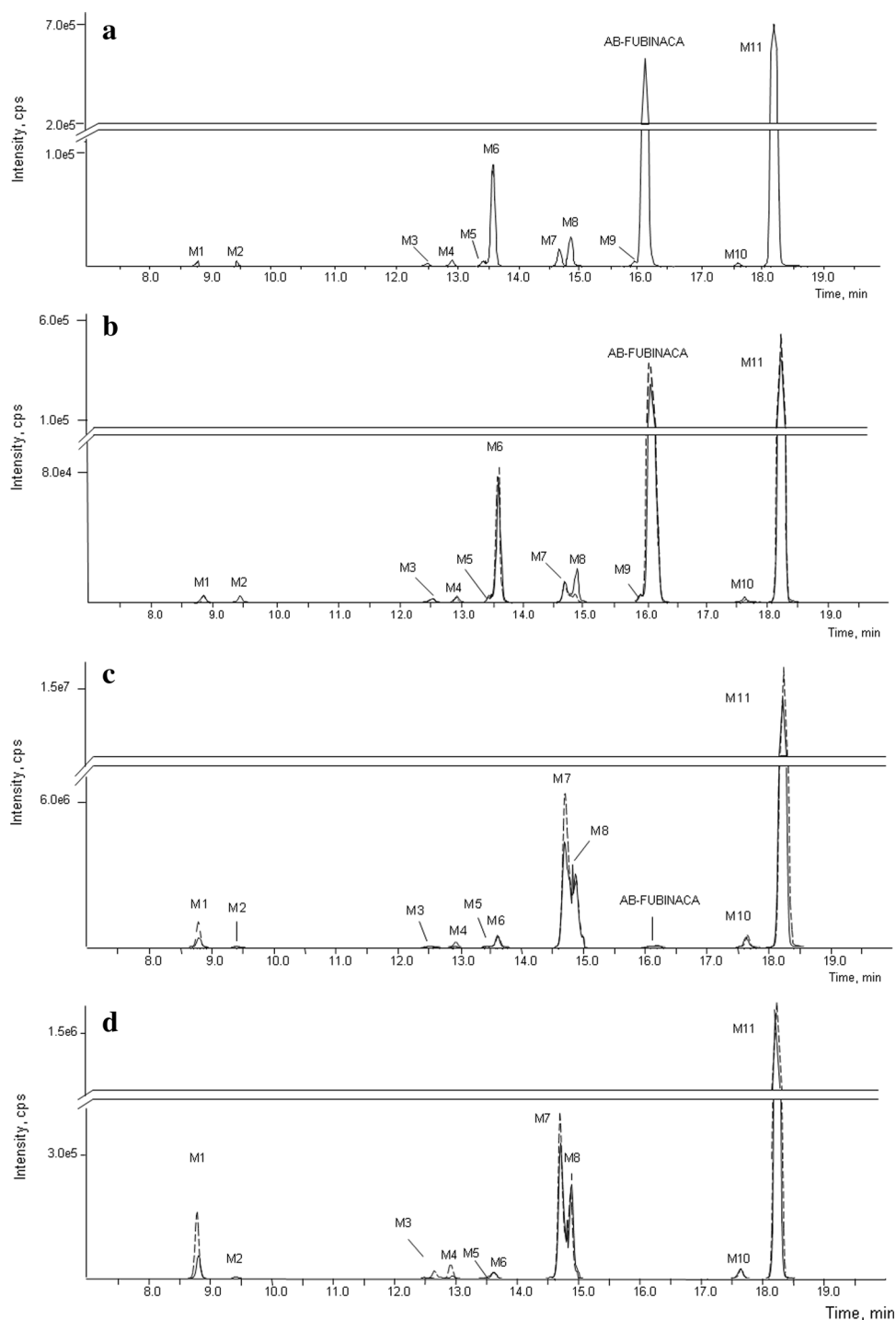
Discussion

Metabolic stability

AB-FUBINACA's half-life was calculated as 62.6 ± 4.0 min, consistent with the moderate 26 and 22 % decrease in peak areas observed after 1 and 3 h of hepatocyte incubation, respectively. Predicted CL_H was 6.9 ml min^{-1} kg^{-1} and the extraction ratio was 0.34. Based on different classifications, the first value would classify AB-FUBINACA as a low-clearance drug, and the second value as an intermediate-clearance drug. According to McNaney et al. [28], drugs with hepatic clearance below 15 ml min^{-1} kg^{-1} are low clearance drugs, while Lave et al. [29] placed drugs with an extraction ratio between 0.3 and 0.7 in the intermediate category. As a result, we

Table 2 Analysis of hepatocyte samples and authentic urine specimens associated with AB-FUBINACA intake

ID	Metabolic reaction(s)	RT (min)	Hepatocyte samples at 3 h			Specimen 1		Specimen 2	
			1:5 Dilution (rank)	SLE+ (rank)	Hydrolysis + SLE+ (rank)	SLE+ (rank)	Hydrolysis + SLE+ (rank)	SLE+ (rank)	Hydrolysis + SLE+ (rank)
M1	Epoxide hydrolysis	8.81	1.41E+04 (7)	1.12E+04 (7)	1.41E+04 (5)	1.40E+06 (6)	3.70E+06 (4)	1.85E+05 (4)	5.20E+05 (4)
M2	Hydroxylation + glucuronidation	9.44	1.31E+04 (9)	9.56E+03 (9)	ND	2.59E+05 (7)	ND	4.27E+04 (7)	ND
M3	Dihydroxylation	12.57	7.06E+03 (11)	4.08E+03 (11)	3.83E+03 (10)	8.26E+04 (9)	1.03E+05 (8)	5.97E+03 (9)	1.24E+04 (8)
M4	Hydroxylation	12.98	1.64E+04 (5)	1.08E+04 (8)	1.36E+04 (6)	8.32E+04 (8)	8.49E+05(7)	1.68E+04 (8)	1.40E+05 (5)
M5	Hydroxylation	13.49	1.50E+04 (6)	1.19E+04 (6)	1.31E+04 (7)	6.50E+04 (10)	9.13E+04 (9)	1.87E+03 (10)	3.21E+03 (9)
M6	Hydroxylation	13.65	3.41E+05 (3)	2.82E+05 (2)	3.38E+05 (2)	2.28E+06 (4)	2.15E+06 (5)	5.75E+04 (6)	7.26E+04 (7)
M7	Hydroxylation + amide hydrolysis	14.73	4.38E+04 (4)	3.44E+04 (4)	4.11E+04 (3)	1.87E+07 (3)	2.79E+07 (2)	1.07E+06 (3)	1.21E+06 (2)
M8	Amide hydrolysis + glucuronidation	14.84	3.48E+05 (2)	8.13E+04 (3)	4.06E+04 (4)	2.84E+07 (2)	2.64E+07 (3)	1.34E+06 (2)	9.81E+05 (3)
M9	Dehydrogenation	15.96	1.37E+04 (8)	1.25E+04 (5)	1.27E+04 (8)	ND	ND	ND	ND
M10	Amide hydrolysis + dehydrogenation	17.67	8.81E+03 (10)	7.33E+03 (10)	9.44E+03 (9)	1.94E+06 (5)	2.03E+06 (6)	9.87E+04 (5)	9.07E+04 (6)
M11	Amide hydrolysis	18.27	3.15E+06 (1)	2.38E+06 (1)	2.78E+06 (1)	1.08E+08 (1)	1.40E+08 (1)	6.15E+06 (1)	7.27E+06 (1)
	Parent	16.14	2.52E+06	2.00E+06	2.37E+06	2.68E+05	2.68E+05	ND	ND

Two authentic urine samples (specimens 1 and 2), with or without hydrolysis, were subjected to supported liquid extraction (SLE+) and analyzed by the high-resolution mass spectrometry. Metabolite peak areas were quantified by MultiQuant and ranked from the most abundant to least abundant peak areas. Peak areas for M8's co-eluting isomers were quantified conjointly. Each sample was analyzed once.

ND not detected

Table 3 Top 20 most intense AB-FUBINACA metabolites identified in two authentic urine specimens with matching blood specimens positive for AB-FUBINACA

Peak ID	Metabolic reaction(s)	Elemental composition	$[M + H]^+$	Mass error (ppm)	RT (min)	Specimen 1		Specimen 2	
						SLE+ (rank)	Hydrolysis + SLE+ (rank)	SLE+ (rank)	Hydrolysis + SLE+ (rank)
a	N-Dealkylation of fluorobenzyl + hydroxylation	$C_{13}H_{16}N_4O_3$	277.1296	0.4	5.47	7.25E+06 (5)	8.02E+06 (6)	6.04E+05 (4)	5.79E+05 (6)
b	N-Dealkylation of fluorobenzyl + dehydrogenation	$C_{13}H_{14}N_4O_2$	259.1192	1.1	5.51		1.44E+06 (18)		2.02E+05 (9)
c	Epoxide hydrolysis + hydroxylation	$C_{20}H_{23}N_4O_5F$	419.1728	0.8	6.12	1.93E+06 (12)	1.88E+06 (15)	2.14E+05 (9)	7.35E+05 (4)
M1	Epoxide hydrolysis	$C_{20}H_{23}N_4O_4F$	403.1775	−0.2	8.78	1.99E+06 (11)	5.48E+06 (7)	2.59E+05 (7)	1.95E+05 (10)
d	Amide hydrolysis + hydroxylation	$C_{20}H_{20}N_3O_4F$	386.1501	−2.4	8.79				1.71E+05 (12)
e	N-Dealkylation of aminooxobutane + hydroxylation	$C_{15}H_{12}N_3O_2F$	286.0983	−1.3	9.41			8.71E+04 (12)	1.04E+05 (17)
f	Dihydroxylation	$C_{20}H_{21}N_4O_4F$	401.1616	−1.0	10.40				
g	Amide hydrolysis + epoxide hydrolysis	$C_{20}H_{22}N_3O_5F$	404.1612	−1.0	10.60	2.51E+07 (3)	2.54E+07 (4)	3.90E+05 (5)	4.32E+05 (8)
h	N-Dealkylation of aminooxobutane + hydroxylation	$C_{15}H_{12}N_3O_2F$	286.0979	−2.6	11.25		1.55E+06 (17)		1.27E+05 (15)
i	Dihydroxylation	$C_{20}H_{21}N_4O_4F$	401.1606	−3.5	11.27				
j	Internal amide hydrolysis (intact indazole)	$C_{15}H_{11}N_2O_2F$	271.0882	1.8	11.28	2.23E+06 (9)		6.84E+04 (18)	9.45E+04 (20)
k	Amide hydrolysis + hydroxylation + glucuronidation	$C_{26}H_{28}N_3O_{10}F$	562.1825	−1.2	12.03	9.72E+05 (19)			
l	Amide hydrolysis + hydroxylation + glucuronidation	$C_{26}H_{28}N_3O_{10}F$	562.1823	−1.5	12.19	1.79E+06 (13)			
m	Carboxylation	$C_{20}H_{19}N_4O_4F$	399.1459	−1.1	12.64			7.20E+04 (17)	
n	Amide hydrolysis + hydroxylation + glucuronidation	$C_{26}H_{28}N_3O_{10}F$	562.1823	−1.4	12.65	1.34E+06 (16)	1.70E+06 (16)	1.03E+05 (11)	1.01E+05 (19)
o	Amide hydrolysis + dihydroxylation	$C_{20}H_{20}N_3O_5F$	402.1459	−0.3	12.76	1.04E+06 (17)		7.57E+04 (15)	
p	Amide hydrolysis + hydroxylation + glucuronidation	$C_{26}H_{28}N_3O_{10}F$	562.1825	−1.1	12.82	7.09E+06 (6)		2.30E+05 (8)	1.52E+05 (14)
q	Amide hydrolysis + hydroxylation + glucuronidation	$C_{26}H_{28}N_3O_{10}F$	562.1840	1.5	12.91		3.39E+06 (10)		
M4	Hydroxylation	$C_{20}H_{21}N_4O_3F$	385.1669	−0.4	12.91	1.77E+06 (14)			1.74E+05 (11)
r	Glucuronidation	$C_{26}H_{29}N_4O_8F$	545.2030	−2.2	12.92				
s	Internal carboxamide hydrolysis + hydrogenation	$C_{15}H_{13}N_2OF$	257.1081	−1.4	13.37		5.12E+06 (8)		7.21E+05 (5)
M6	Hydroxylation	$C_{20}H_{21}N_4O_3F$	385.1669	−0.4	13.60	2.73E+06 (7)	2.70E+06 (14)	6.61E+04 (19)	1.65E+05 (13)
t	N-Dealkylation of C_5H_9NO	$C_{15}H_{12}N_3OF$	270.1033	−1.5	14.01	1.01E+06 (18)	1.36E+06 (20)	7.56E+04 (16)	
u	Amide hydrolysis + hydroxylation	$C_{20}H_{20}N_3O_4F$	386.1505	−1.6	14.17	2.13E+06 (10)	2.90E+06 (11)	8.59E+04 (13)	
v	Amide hydrolysis + glucuronidation (M8 isomer 4)	$C_{26}H_{28}N_3O_9F$	546.1888	1.1	14.26	8.37E+05 (20)			
w	Internal amide hydrolysis (indazole remaining) + hydroxylation	$C_{15}H_{11}N_2O_2F$	271.0875	−0.8	14.42		3.88E+06 (9)	8.38E+04 (14)	
M7	Amide hydrolysis + hydroxylation	$C_{20}H_{20}N_3O_4F$	386.1510	−0.1	14.69	2.41E+07 (4)	3.72E+07 (3)	1.51E+06 (3)	1.75E+06 (2)

Table 3 continued

Peak ID	Metabolic reaction(s)	Elemental composition	$[M + H]^+$	Mass error (ppm)	RT (min)	Specimen 1		Specimen 2	
						SLE+ (rank)	Hydrolysis + SLE+ (rank)	SLE+ (rank)	Hydrolysis + SLE+ (rank)
M8	Amide hydrolysis + glucuronidation	$C_{26}H_{28}N_3O_9F$				4.8E+07[a] (2)	5.08E+07[a] (2)	2.06E+06[a] (2)	1.64E+06[a] (3)
	(isomer 1)		546.1875	−1.4	14.78				
	(isomer 2)		546.1895	2.3	14.87				
	(isomer 3)		546.1862	−3.7	15.10				
x	Amide hydrolysis + hydroxylation	$C_{20}H_{20}N_3O_4F$	386.1524	3.4	14.88		9.87E+06 (5)	3.45E+05 (6)	4.36E+05 (7)
y	Amide hydrolysis + hydroxylation	$C_{20}H_{20}N_3O_4F$	386.1521	2.7	15.93		2.78E+06 (12)		
z	Amide hydrolysis + dehydrogenation	$C_{20}H_{18}N_3O_3F$	368.1403	−0.5	17.38	1.72E+06 (15)	1.41E+06 (19)		1.03E+05 (18)
M10	Amide hydrolysis + dehydrogenation	$C_{20}H_{18}N_3O_3F$	368.1405	−0.1	17.62	2.53E+06 (8)	2.76E+06 (13)	1.21E+05 (10)	1.16E+05 (16)
M11	Amide hydrolysis	$C_{20}H_{20}N_3O_3F$	370.1562	0	18.21	1.31E+08 (1)	1.70E+08 (1)	7.90E+06 (1)	9.20E+06 (1)

Metabolites previously identified in hepatocytes were assigned by the corresponding ID, and additional metabolites were assigned alphabetically in order of their RTs. Peak areas for metabolites not in the top 20 were not listed; conversely, blank peak areas do not necessarily represent undetected metabolites. Each sample was analyzed once.

[a] M8 combined peak areas for isomer 1, 2 and 3; $[M + H]^+$, protonated molecule

assume that metabolites generated from AB-FUBINACA can be seen in urine for a few days post-dosing.

Identification of AB-FUBINACA metabolites after human hepatocyte incubation

AB-FUBINACA fragmentation pattern

We observed four distinct product ions for AB-FUBINACA (Fig. 4). Bond cleavage between the carbon and nitrogen of the internal carboxamide group produced the most intense fragment, m/z 253. Removal of the terminal carboxamide yielded m/z 324; m/z 109 was associated with the 4-fluorobenzyl substructure, and cleavage between the carboxamide carbon and nitrogen atom produced m/z 352. Interestingly, no fragment at m/z 145, theoretically corresponding to the indazole acylium ion, was observed, which might be caused by fluorobenzyl being an excellent leaving group. The unique fragmentation pattern of AB-FUBINACA was utilized for metabolite detection (via the product ion filter or neutral loss filter) as well as metabolite structural elucidation.

Metabolites generated by carboxamide hydrolysis

AB-FUBINACA carboxylic acid (M11), a product of terminal carboxamide hydrolysis, was the most intense metabolite observed in 1 and 3-h hepatocyte samples (Table 1; Fig. 2), which is consistent with Thomsen et al.'s [26] findings. Figure 4 depicts product ion spectra of all eleven metabolites identified in hepatocytes. M11 product ion spectrum showed three distinct fragments of the native AB-FUBINACA molecule (m/z 109, 253, and 324) suggesting no modification at these areas of the molecule. To compare our HLM findings with Takayama et al.'s [16], we re-analyzed our samples by the previous HLM LC–MS-MS method that had been updated to include MRM transitions for all metabolites identified in the hepatocytes. We found M11 was the most predominant metabolite in our HLM samples and should have been detectable in Takayama et al.'s [16] experiment. Further glucuronidation of M11 yielded M8 at m/z 546. M8 product ion spectrum showed a characteristic fragment at m/z 370, which was produced by cleavage of glucuronic acid, and the same three distinct fragments of AB-FUBINACA carboxylic acid (m/z 109, 253, and 324).

M7 was a product of amide hydrolysis and further hydroxylation at the aminooxobutane moiety as suggested by the presence of m/z 109, 253 and 350. The first two fragments correspond to an unchanged fluorobenzyl indazole structure, leaving the modifications to the remaining parts of the molecule. However, the exact position of the hydroxyl group at the aminooxobutane moiety is unclear.
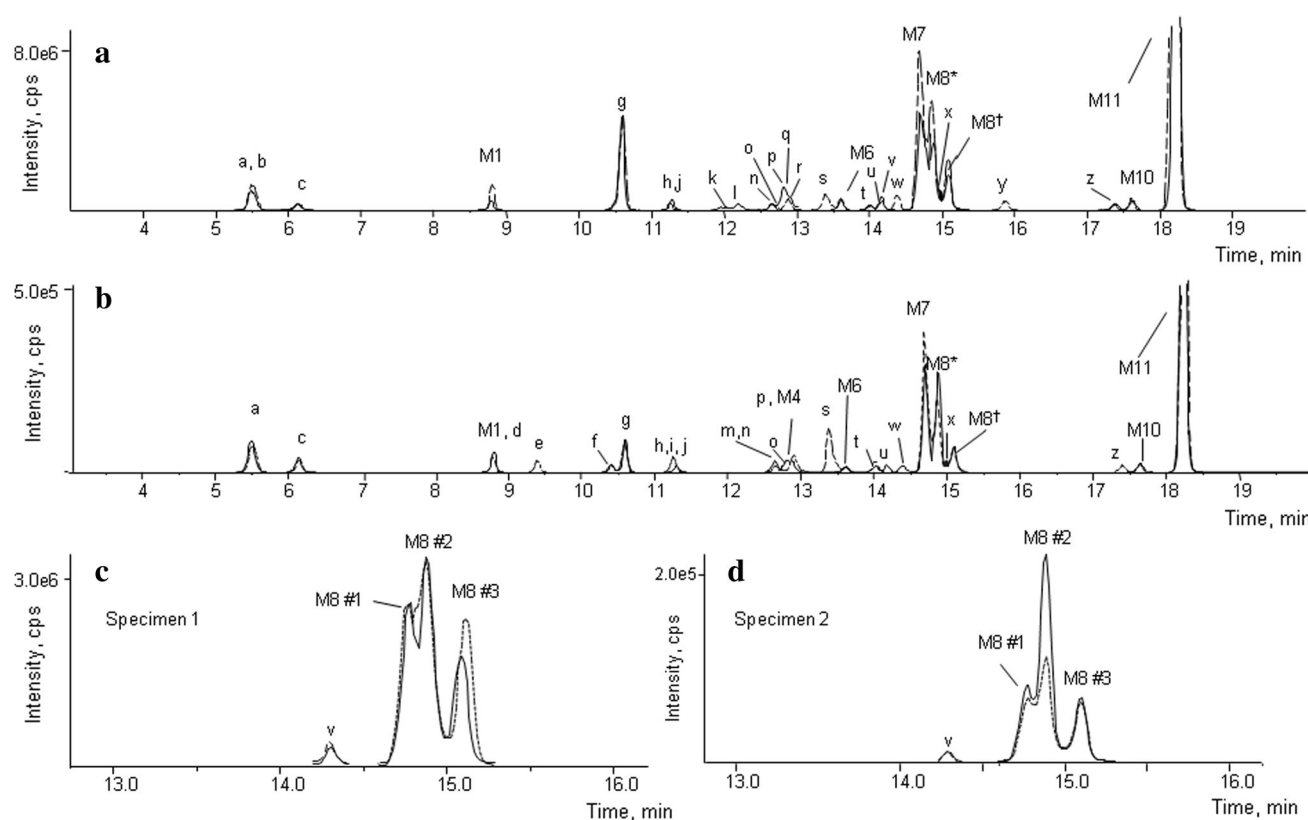
Fig. 3 Combined extracted ion chromatograms of the top 20 most intense AB-FUBINACA metabolites identified in urine specimen 1 (**a**) and specimen 2 (**b**). Specimens, with or without enzyme hydrolysis treatment, were further subjected to solid-supported liquid extraction (SLE+) prior to analysis. Metabolites identified after hydrolysis are represented by broken lines. Extracted ion chromatograms for the acyl glucuronide metabolite M8 (**c**, **d**), which has four isomers: three shown as clusters and metabolite "v" with identical product ion mass spectra in the unhydrolyzed samples. M8* denotes isomers 1 and 2 co-eluting while M8[†] represents isomer 3. M11 maximum peak heights in unhydrolyzed/hydrolyzed specimen 1 (**a**) was 1.5E+7/2.0E+7 and in specimen 2 (**b**) 1.5E+6

Most likely, M7 was mainly formed by amide hydrolysis of M6 since M6 was major in hepatocytes (Fig. 2a, b) and minor in human urine (Fig. 2c, d) while M7 was minor in hepatocytes and major in urine. M10 is a metabolite generated by combined amide hydrolysis and dehydrogenation at the aminooxobutane moiety. Characteristic fragments were m/z 109, 253, 322, and 350.

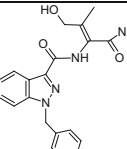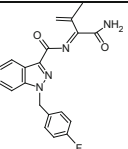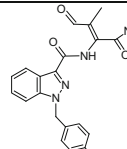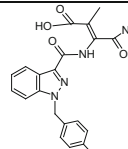*Metabolites generated by hydroxylations*
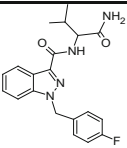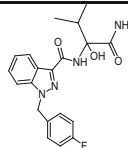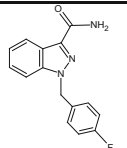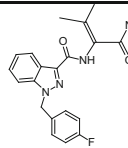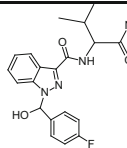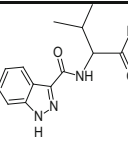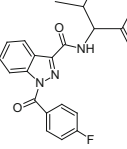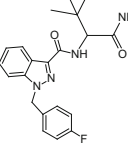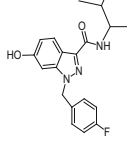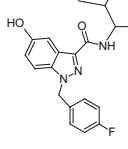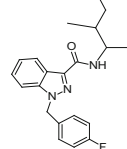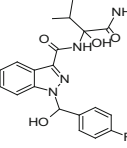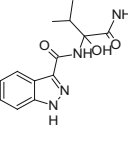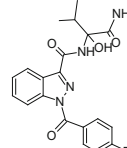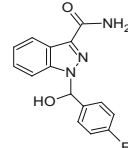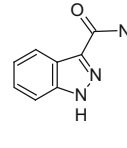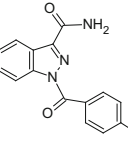
Three monohydroxylated metabolites (M4, M5, and M6), one dihydroxylated metabolite (M3) and a further glucuronidated monohydroxylated metabolite (M2) were identified. Hydroxylations occurred at different sites of the molecule, but predominantly at the aminooxobutane moiety. M6 was the second most intense peak after 1 and 3 h incubation showing fragments at m/z 109, 253, 310, 340, and 368 that suggest hydroxylation at the aminooxobutane moiety. The exact position of the hydroxyl group is unclear, although in silico prediction proposes hydroxylation at the 2″-position (P1) with the highest possible score of 100 %. M6 might correspond to the single AB-FUBINACA monohydroxylated metabolite that Takayama et al. [16] identified in their HLM experiment and to M4 in Thomsen et al.'s study [26]. Eluting closely and showing the same fragments, M5 is another metabolite monohydroxylated at the aminooxobutane moiety. The dihydroxylated metabolite M3 showed fragments at m/z 109, 253, 326, 356, 366, and 384, which are consistent with two hydroxyl groups at the aminooxobutane moiety.

In contrast, M4 product ion spectrum showed a distinct fragment at m/z 269, which was not observed for M5 or M6 and suggests that hydroxylation occurred on the indazole moiety with m/z fragment 109 still intact. As for all unassigned hydroxyl positions, further analysis with nuclear magnetic resonance or testing reference standards is necessary to confirm the exact structure.

The glucuronidated monohydroxylated metabolite M2 was hydroxylated on either the indazole or methylene carbon of the fluorobenzyl moiety (m/z 269) and might be the phase II metabolite of M4 as the peak area increased after hepatocyte sample hydrolysis while M2 was undetected. The distinct fragment m/z 445 was generated by

Table 4 In silico metabolite prediction of AB-FUBINACA metabolites by MetaSite™ software

First generation	AB-FUBINACA	P1	P2	P3	P4	P5
Biotransformation	Parent	Hydroxylation	*N*-Dealkylation	Dehydrogenation	Hydroxylation	*N*-Dealkylation
Mass (Da)	368.1685	384.1598	269.0964	366.1492	384.1598	260.1273
LogD4	2.94	2.40	2.45	2.59	2.37	1.15
Probability Score,%	Not applicable	100	100	100	73	73

	P6	P7	P8	P9	P10
Biotransformation	Carbonylation	Hydroxylation	Hydroxylation	Hydroxylation	Hydroxylation
Mass (Da)	382.1142	384.1598	384.1598	384.1598	384.1598
LogD4	2.65	1.65	2.53	2.53	1.76
Probability Score,%	73	47	27	24	20

Second generation	P1a	P1b	P1c	P2a	P2b	P2c
Biotransformation	Hydroxylation	*N*-Dealkylation	Carbonylation	Hydroxylation	*N*-Dealkylation	Carbonylation
Mass (Da)	400.1546	276.1222	389.1390	285.0913	161.0589	283.0757
LogD4	1.82	0.6	2.10	1.87	0.6	2.16
Probability Score,%	100	100	100	100	100	100

	P3a	P3b	P3c	P3d
Biotransformation	Hydroxylation	Dehydrogenation	Carbonylation	Carboxylation
Mass (Da)	382.1441	364.1335	380.1284	396.1233
LogD4	1.15	3.54	0.75	0.80
Probability Score,%	100	100	100	100

Metabolites are ranked according to their probability score

cleavage of the internal carboxamide splitting off the aminooxobutane moiety. This supports our assumption that glucuronidation did not occur at this substructure.

Metabolites generated by dehydrogenation and epoxide hydrolysis

AB-FUBINACA also underwent other biotransformations, e.g., dehydrogenation and epoxidation followed by hydrolysis. We suggest that M9, a minor metabolite with fragments at *m/z* 109, 253, 322, and 350, is dehydrogenated. We did not observe any indication that this metabolite might be an artifact created by water loss during ionization as there was no co-eluting corresponding metabolite. The exact double bond location cannot be definitely determined; however, MetaSite™ proposes de-hydrogenation at the 2″-position (P3) with a probability score of 100 % (Table 4).
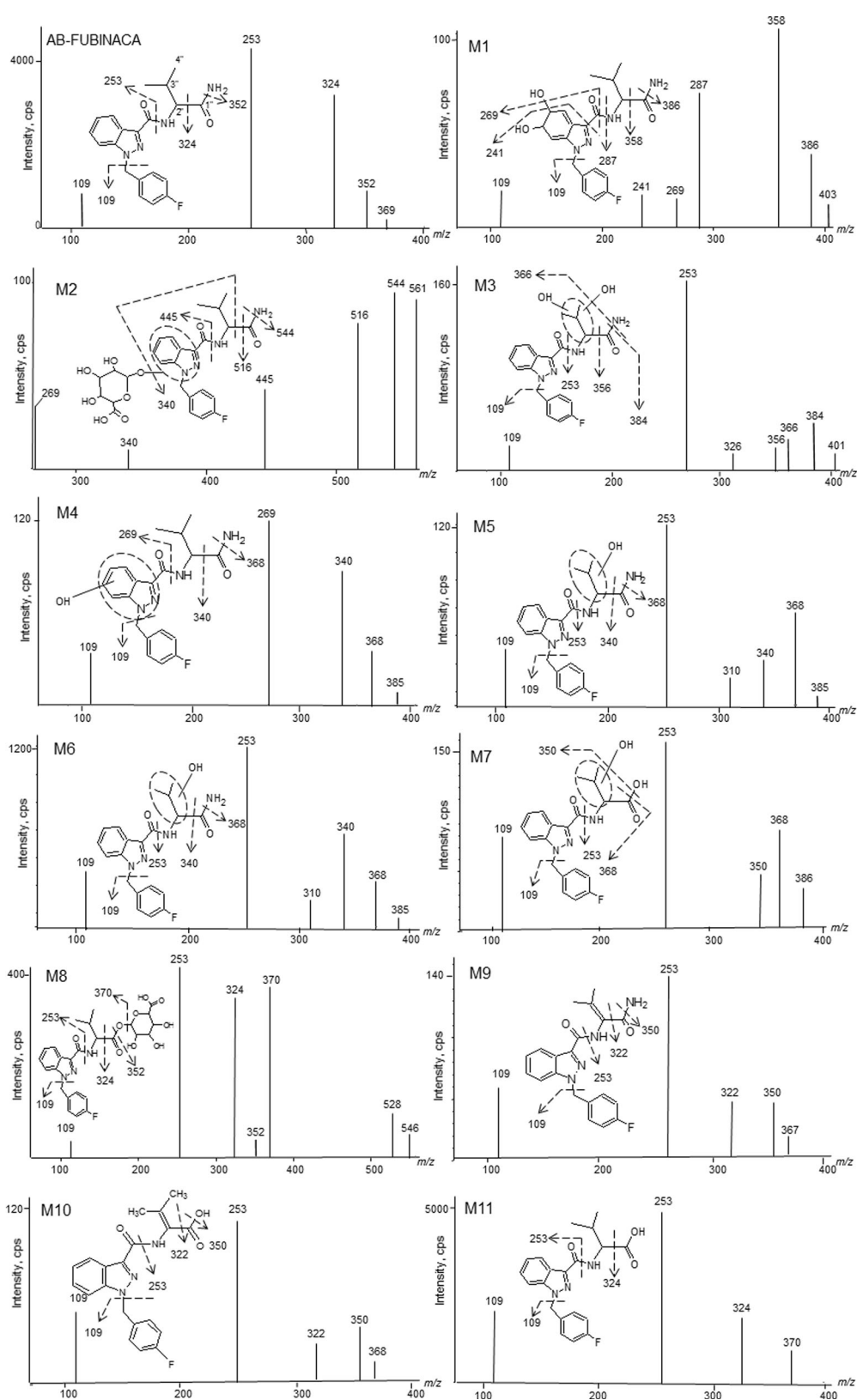
Fig. 4 Product ion mass spectra and assigned fragmentation pattern for AB-FUBINACA and all metabolites that were identified after human hepatocyte incubation. *Markush bond* indicates unassigned hydroxy position. The exact location of the dihydrodiol structure at the indazole moiety (M1) is not clear

As observed with AM2201 [30] and PB-22 [22], epoxide hydrolysis to a dihydrodiol structure occurred for AB-FUBINACA producing M1. The characteristic fragments at m/z 109, 241, 269, 287, and 358 are consistent with AB-FUBINACA undergoing this two-step reaction, epoxide formation and subsequent hydrolysis, to produce a dihydrodiol at the indazole core at several possible sites.

Prevalence of AB-FUBINACA metabolites

Among the nine phase I metabolites in human hepatocyte samples, AB-FUBINACA carboxylic acid (M11) was the predominant metabolite at both time points followed by hydroxy AB-FUBINACA (M6) and AB-FUBINACA carboxylic acid glucuronide (M8). M11 and M6 also were the most intense metabolites in our HLM samples, where we additionally identified M4 and M7 with a ten-fold lower intensity. These are more metabolites than Takayama et al. [16] found, but less than in Thomsen et al.'s study [26]. However, the latter group incubated for 3 h instead of 1 h. We determined AB-FUBINACA metabolite prevalence based on peak areas, which could be influenced by matrix effects and different ionization efficiencies for different molecular structures. Nevertheless, it is possible to characterize AB-FUBINACA metabolite prevalence in vitro based on MS data. The proposed AB-FUBINACA metabolic pathway is illustrated in Fig. 5.

Metabolite profiles in authentic human urine specimens

Analogous to the hepatocyte samples, AB-FUBINACA carboxylic acid (M11) was the predominant metabolite in authentic urine samples with or without β-glucuronidase treatment. Equally important, all metabolites but one that were previously identified in the hepatocyte samples were also observed in both urine samples (Fig. 2c, d), confirming the utility of hepatocytes for in vivo metabolite prediction. However, there was a shift towards second-generation metabolites; instead of M6 (ranked #2 in hepatocytes), M7 and M8 (ranked #4 and #3 in hepatocytes, respectively) dominated in the hydrolyzed urine specimens. As described above, M7 probably started as M6 and further underwent amide hydrolysis (or the other way round). Definitely, M8 is the phase II metabolite of M11. Information regarding AB-FUBINACA dose, intake frequency, and collection time of our samples were unknown. Thus, it is possible that the urinary profiles we obtained represent a later time point in the metabolism than the 3 h hepatocyte profile, or are results of multiple intakes. The first hypothesis is supported by the fact that we identified additional metabolites in the urine samples (Fig. 3), suggesting more extensive AB-FUBINACA metabolism.

When considering all metabolites present, six and seven metabolites identified in the hepatocyte sample were also among the top 20 AB-FUBINACA metabolites in urine specimen 1 and 2, respectively. Moreover, M11, M7, and M8 remained the top three most intense metabolites in both specimens. Only one additional metabolite–metabolite "g" in specimen 1, generated by epoxide hydrolysis and amide hydrolysis–reached similar intensity. The consistency of in vitro and in vivo major metabolic pathways for AB-FUBINACA, again, confirms the usefulness of hepatocytes for in vivo predictions. Although the metabolic rate in HLMs was low, oxidative metabolism rather than direct elimination of the parent was the major clearance pathway. These findings taken together lead us to expect a detection window in the range of days for the metabolites in urine.

Interestingly, we observed a cluster consisting of at least three peaks in the chromatogram for the acyl glucuronide M8 at 14.7–15.1 min (Table 3; Fig. 3c, d), each peak at m/z 546.18 yielding identical MS-MS spectra. M8 was deemed an acyl glucuronide since multiple isomers of M8 were observed in human urine specimens, probably formed after keeping them at room temperature for several hours. Acyl glucuronides are commonly observed conjugates of carboxylic acid-containing compounds [31] and are electrophilic and highly reactive compounds. The rate of acyl glucuronide isomer formation from non-enzymatic intramolecular rearrangement is influenced by pH and temperature; some isomers may be resistant to beta-glucuronidase hydrolysis [31]. This could explain why peak 2 decreased after enzymatic hydrolysis, whereas peaks 1 and 3 did not. We also observed a 4th peak for m/z 546.188 at 14.26 min with product ion mass spectra identical to M8 in both urine specimens; however, this metabolite was only in the top 20 before hydrolysis of specimen 1. Although acyl glucuronide metabolites may form protein adducts resulting in drug-drug interactions and potential hepatoxicity [31], further research on AB-FUBINACA acyl glucuronide adducts is needed to confirm that.

Amide hydrolysis appears to be a major elimination pathway with the majority of the top 20 prevalent metabolites being second-generation products of amide hydrolysis. Another common biotransformation was N-dealkylation of the fluorobenzyl ring producing metabolites missing a characteristic part of the AB-FUBINACA molecule. These metabolites are potentially shared with other synthetic cannabinoids (e.g., AB-PINACA and AB-CHIMINACA), making them less valuable for forensic interpretations.

Interestingly, AB-FUBINACA itself was detected in urine specimen 1 that had a matching whole blood specimen containing 42 ng/g of AB-FUBINACA. Parent synthetic cannabinoids are typically not found in urine due to instability and/or extensive metabolism [32, 33]. Collection

Fig. 5 Proposed metabolic pathway of AB-FUBINACA in human hepatocytes. Unassigned hydroxy positions are depicted as Markush structures. The exact location of the dihydrodiol structure of M1 is not clear. Based on the changes in peak areas observed in the hepatocyte and urine specimens, M7 was probably generated from M6. Assignment of the exact location of the hydroxy group in M4 and M2 is unclear, which is why it cannot be definitely determined that M2 is generated from M4
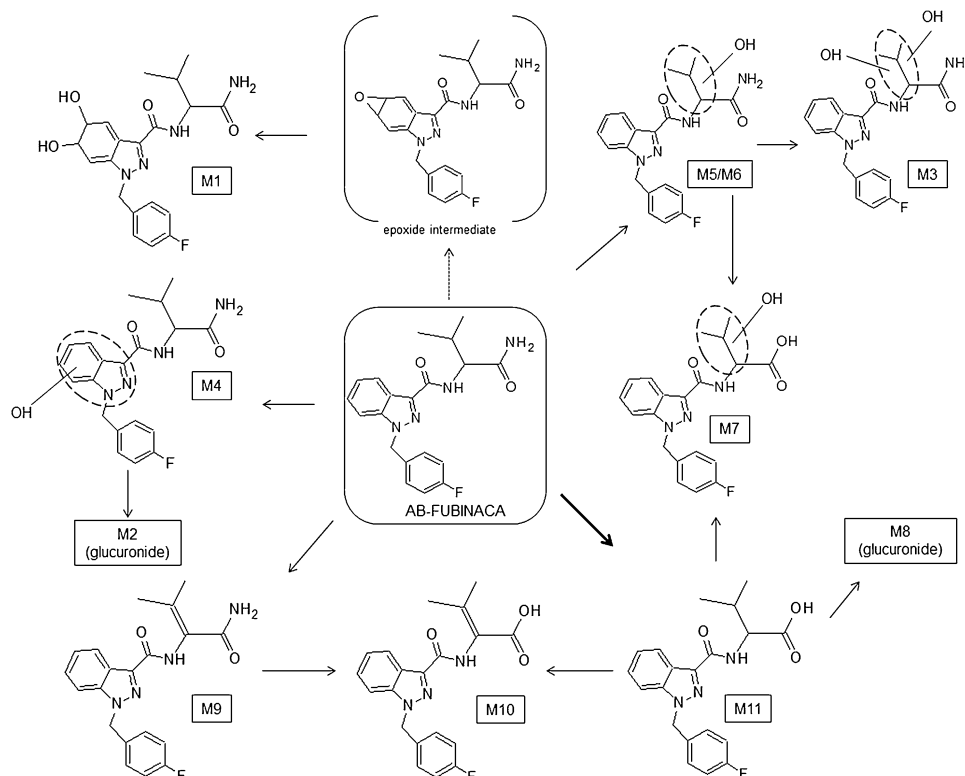
time, drug dose and frequency and storage conditions can all affect AB-FUBINACA detectability in urine.

Another interesting observation is the absence of defluorinated metabolites in both hepatocyte and authentic urine specimens. This is in contrast to many fluoropentyl indole/indazole synthetic cannabinoids, for which aliphatic defluorination was a major metabolic pathway [17, 18, 24]. Our results suggest that aromatic defluorination of AB-FUBINACA does not occur.

We propose M11 and M7 as suitable phase I AB-FUBI-NACA urinary markers, as these were predominant in hepatocytes and authentic urine specimens. We also suggest M1 or M6, metabolites with intact terminal carboxamide groups, as the most effective metabolites for clearly determining AB-FUBINACA intake during urine drug testing.

In silico prediction of AB-FUBINACA metabolites

Metabolite prediction software predicts potential metabolites independent of in vitro or in vivo experiments. We used the commercially available software (MetaSite[TM]) to predict metabolites and to evaluate how well the predictions match the in vitro/in vivo results. It is important to remember that MetaSite[TM] is capable of predicting phase I metabolites generated by CYP450 and FMO3 biotransformations only, implying that any metabolites generated by other enzymes, e.g., carboxylesterases, will be missed.

Therefore, the most intense metabolite M11 (and all metabolites derived from it) will not be among the predicted metabolites [26]. We identified nine phase I metabolites in our 3-h hepatocyte samples, of which six qualified for being predicted, ranking M6 ≫ M4 > M1, M9, M5 > M3. M6 might correspond to predicted metabolite P1 that scored 100 %; M4 to P4, P8 or P9; M9 to P3 that scored 100 %; M5 to P1, but more likely P7 or P10. The dihydrodiol structure in M1 was not predicted. For final evaluation of the software's accuracy, exact metabolite structures are needed.

Conclusions

We identified 11 AB-FUBINACA metabolites in our human hepatocyte samples with AB-FUBINACA carboxylic acid (M11), hydroxy-aminooxobutane AB-FUBINACA (M6), and AB-FUBINACA carboxylic acid glucuronide (M8) being the most intense. In authentic urine specimens, AB-FUBINACA carboxylic acid (M11), hydroxy-aminooxobutane AB-FUBINACA carboxylic acid (M7), and AB-FUBINACA carboxylic acid glucuronide (M8) were the three most prevalent metabolites and are recommended as suitable urinary markers for AB-FUBINACA intake. M1 and M6 also could be helpful. In brief, the major metabolic pathways of AB-FUBINACA in human

in vitro and in vivo were consistent. Although AB-FUBI-NACA had low to medium clearance in HLMs, low concentrations of the parent drug were identified in human urine. Biotransformations to M11 and M6 were major drug clearance pathways. It is expected that M11, M6 and/or their further metabolites, M7 and M8, can be present in urine a few days post intake.

Conflict of interest There are no financial or other relations that could lead to a conflict of interest.

Ethical approval This article does not contain any studies with human or animal subjects performed by any of the authors.

References

1. Castaneto MS, Gorelick DA, Desrosiers NA, Hartman RL, Pirard S, Huestis MA (2014) Synthetic cannabinoids: epidemiology, pharmacodynamics, and clinical implications. Drug Alcohol Depend 144:12–41

2. United Nations on Drugs and Crime. World Drug Report 2014 (2014) United Nations: Vienna.http://www.unodc.org/documents/wdr2014/World_Drug_Report_2014_web.pdf. Accessed Dec 2014

3. US Drug Enforcement Administration (2013) Establishment of drug codes for 26 substances. Final rule. Fed Regist 78:664–666

4. Buchler JP, Hayes MJ, Hegde SG, Hockerman SL, Jones DE, Kortum SW, Rico JG, Tenbrink RE, Wu KK (2009) Indazole derivatives. US Patent CA 2714573 A1:1–283

5. Brents LK, Reichard EE, Zimmerman SM, Moran JH, Fantegrossi WE, Prather PL (2011) Phase I hydroxylated metabolites of the K2 synthetic cannabinoid JWH -018 retain in vitro and in vivo cannabinoid 1 receptor affinity and activity. PLoS One 6:e21917

6. Uchiyama N, Matsuda S, Wakana D, Kikura-Hanajiri R, Goda Y (2013) New cannabimimetic indazole derivatives, N-(1-amino-3-methyl-1-oxobutan-2-yl)-1-pentyl-1H-indazole-3-carboxamide (AB-PINACA) and N-(1-amino-3-methyl-1-oxobutan-2-yl)-1-(4-fluorobenzyl)-1H-indazole-3-caboxamide (AB-FUBINACA) identified as designer drugs in illegal products. Forensic Toxicol 31:93–100

7. Drug Enforcement Administration (2014) 2013 Midyear Report. Department of Justice, Springfield, VA. http: http://www.deadiversion.usdoj.gov/nflis/2013midyear.pdf. Accessed Aug 2014

8. Drug Enforcement Administration (2014) Schedules of controlled substances: temporary placement of four synthetic cannabinoids into schedule I: notice of intent. Fed Regist 79:7577–7582

9. Centers for Disease Control and Prevention (2013) Notes from the field: severe illness associated with synthetic cannabinoid use—Brunswick, Georgia, 2013. MMWR Morb Mortal Wkly Rep 62:939

10. Federal Drug Control Service of Russia (2014) Выступление председателя ГАК, директора ФСКН России В.П. Иванова на заседании ГАК 6 октября 2014 г. http://fskn.gov.ru/includes/periodics/speeches_fskn/2014/1006/124332682/detail.shtml. Accessed Dec 2014

11. Gurney SMR, Scott KS, Kacinko SL, Presley BC, Logan BK (2014) Pharmacology, toxicology, and adverse effects of synthetic cannabinoid drugs. Forensic Sci Rev 26:53–78

12. Research Chemical Review (2014) Trip report tme: 250 mg AB-FUBINACA and 500 mg AH-7921. http://researchchemicalreview.wordpress.com/2014/02/25/trip-report-tme-250mg-ab-fubinaca-and-500mg-ah-7921/ Accessed Aug 2014

13. De Brabanter N, Esposito S, Tudela E, Lootens L, Meuleman P, Leroux-Roels G, Deventer K, Van Eenoo P (2013) In vivo and in vitro metabolism of the synthetic cannabinoid JWH-200. Rapid Commun Mass Spectrom 27:2115–2126

14. Grigoryev A, Melnik A, Savchuk S, Simonov A, Rozhanets V (2011) Gas and liquid chromatography-mass spectrometry studies on the metabolism of the synthetic phenylacetylindole cannabimimetic JWH-250, the psychoactive component of smoking mixtures. J Chromatogr B 879:2519–2526

15. Wintermeyer A, Moller I, Thevis M, Jubner M, Beike J, Rothschild MA, Bender K (2010) In vitro phase I metabolism of the synthetic cannabimimetic JWH-018. Anal Bioanal Chem 398:2141–2153

16. Takayama T, Suzuki M, Todoroki K, Inoue K, Min JZ, Kikura-Hanajiri R, Goda Y, Toyo'oka T (2014) UPLC/ESI-MS/MS-based determination of metabolism of several new illicit drugs, ADB-FUBINACA, AB-FUBINACA, AB-PINACA, QUPIC, 5F-QUPIC and alpha-PVT, by human liver microsomes. Biomed Chromatogr 28:831–838

17. Jang M, Shin I, Yang W, Chang H, Yoo HH, Lee J, Kim E (2014) Determination of major metabolites of MAM-2201 and JWH-122 in in vitro and in vivo studies to distinguish their intake. Forensic Sci Int 244:85–91

18. Holm NB, Pedersen AJ, Dalsgaard PW, Linnet K (2015) Metabolites of 5F-AKB-48, a synthetic cannabinoid receptor agonist, identified in human urine and liver microsomal preparations using liquid chromatography high-resolution mass spectrometry. Drug Test Anal 7:199–206

19. Jin MJ, Lee J, In MK, Yoo HH (2013) Characterization of in vitro metabolites of CP 47,497, a synthetic cannabinoid, in human liver microsomes by LC–MS/MS. J Forensic Sci 58:195–199

20. Gandhi AS, Wohlfarth AW, Zhu M, Pang S, Castaneto M, Scheidweiler KB, Huestis MA (2015) High-resolution mass spectrometric metabolite profiling of a novel synthetic designer drug, N-(adamantan-1-yl)-1-(5-fluoropentyl)-1H-indole-3-carboxamide (STS-135), using cryopreserved human hepatocytes and assessment of metabolic stability with human liver microsomes. Drug Test Anal 7:187–198

21. Gandhi AS, Zhu M, Pang S, Wohlfarth A, Scheidweiler KB, Liu HF, Huestis MA (2013) First characterization of AKB-48 metabolism, a novel synthetic cannabinoid, using human hepatocytes and high-resolution mass spectrometry. AAPS J 15:1091–1098

22. Wohlfarth A, Gandhi AS, Pang S, Zhu M, Scheidweiler KB, Huestis MA (2014) Metabolism of synthetic cannabinoids PB-22 and its 5-fluoro analog, 5F-PB-22, by human hepatocyte incubation and high-resolution mass spectrometry. Anal Bioanal Chem 406:1763–1780

23. Wohlfarth A, Pang S, Zhu M, Gandhi AS, Scheidweiler KB, Huestis MA (2014) Metabolism of RCS-8, a synthetic cannabinoid with cyclohexyl structure, in human hepatocytes by high-resolution MS. Bioanalysis 6:1187–2000

24. Wohlfarth A, Pang S, Zhu M, Gandhi AS, Scheidweiler KB, Liu HF, Huestis MA (2013) First metabolic profile of XLR-11, a novel synthetic cannabinoid, obtained by using human hepatocytes and high-resolution mass spectrometry. Clin Chem 59:1638–1648

25. Strano-Rossi S, Anzilotti L, Dragoni S, Pellegrino RM, Goracci L, Pascali VL, Cruciani G (2014) Metabolism of JWH-015, JWH-098, JWH-251, and JWH-307 in silico and in vitro: a pilot study for the detection of unknown synthetic cannabinoids metabolites. Anal Bioanal Chem 406:3621–3636

26. Thomsen R, Nielsen LM, Holm NB, Rasmussen HB, Linnet K (2014) Synthetic cannabimimetic agents metabolized by carboxylesterases. Drug Test Anal. doi:10.1002/dta.1731

27. Baranczewski P, Stanczak A, Sundberg K, Svensson R, Wallin A, Jansson J, Garberg P, Postlind H (2006) Introduction to in vitro estimation of metabolic stability and drug interactions of new chemical entities in drug discovery and development. Pharmacol Rep 58:453–472

28. McNaney CA, Drexler DM, Hnatyshyn SY, Zvyaga TA, Knipe JO, Belcastro JV, Sanders M (2008) An automated liquid chromatography-mass spectrometry process to determine metabolic stability half-life and intrinsic clearance of drug candidates by substrate depletion. ASSAY Drug Dev Technol 6:121–129

29. Lave T, Dupin S, Schmitt C, Valles B, Ubeaud G, Chou RC, Jaeck D, Coassolo P (1997) The use of human hepatocytes to select compounds based on their expected hepatic extraction ratios in humans. Pharm Res 14:152–155

30. Sobolevsky T, Prasolov I, Rodchenkov G (2012) Detection of urinary metabolites of AM-2201 and UR-144, two novel synthetic cannabinoids. Drug Test Anal 4:745–753

31. Regan SL, Maggs JL, Hammond TG, Lambert C, Williams DP, Park DK (2010) Acyl glucuronides: the good, the bad and the ugly. Biopharm Drug Dispos 31:367–395

32. Castaneto MS, Scheidweiler KB, Gandhi A, Wohlfarth A, Klette KL, Martin TM, Huestis MA (2014) Quantitative urine confirmatory testing for synthetic cannabinoids in randomly collected urine specimens. Drug Test Anal. doi:10.1002/dta.1709

33. Hutter M, Broecker S, Kneisel S, Auwarter V (2012) Identification of the major urinary metabolites in man of seven synthetic cannabinoids of the aminoalkylindole type present as adulterants in 'herbal mixtures' using LC-MS/MS techniques. J Mass Spectrom 47:54–65